Analysis Of Delamination Identification Sequence In Multi-Stack Fibre Metal Laminate

S. Sundaravalli[1], M. C. Majumder[2], G. Manikandan[3], G. K. Vijayaraghavan[4]*

[1]MAM College of Engineering, Trichy, India*
[2]National Institute of Technology, Durgapur, India 713 209
[3]Velammal College of Engineering and Technology, Madurai, India
[4] Cauvery College of Engineering and Technology, Trichy, India

Abstract

The paper presents the analysis of delamination identification sequence in various stacks of FML, such as single stack, double stack and triple stack FML under step pulse active thermography in both thermal reflection and thermal through-transmission modes. The study was carried out numerically by artificially implanted delaminations of 10×10mm^2 size at various depths.
The numerical results of delaminations in both double stack and triple stack FML conclude that DE 16, DE 21 and DE 22 in thermal reflection mode could not be identified but they could easily be identified in thermal through-transmission mode. It concludes the near-surface delamination 1 located in single stack FML could be identified first with reduced ΔT than delaminations located in both double stack and Triple stack FML. Thus, the results conclude that SPAT in thermal reflection mode could effectively be applied to investigate the near-surface delaminations for its identification sequence and thermal through-transmission mode could be for deeper delaminations.

Keywords: Step pulsed active thermography (SPAT), NDTE, thermal reflection mode, thermal through-transmission mode, FML, Delaminations, Finite element method, Thermal contrast.

1. Introduction

Composite materials have been the subject of permanent interest of various specialists during the last decades. Firstly, military applications in the aircraft industry triggered off the commercial use of composites after the Second World War [5]. The innovations in the composite area have allowed a significant weight reduction in the structural design. In last decades, aircraft panels were manufactured using metallic materials, such as aluminum, titanium, beryllium etc. The use of metallic aircraft panels increased fuel consumption due to more weight [21]. The combination of metallic materials with fibre reinforced polymers into aircraft structural materials is commonly denoted as hybrid concepts or technologies [19]. Therefore, the concept of effective and efficient usage of materials in manufacturing of aircraft panels was slowly emerged by using alloys of metals with offered advantages of reduced weight and cost. The practical difficulties involved in manufacturing alloys of metallic materials. It motivated researchers to keep one step forward in using alternate materials with reduced weight and cost effective, namely, composite materials. The composite materials play an important role in heavy duty applications because of reduction in weight and cost-effective [24]. In 1980s, the Delft University of Technology developed a new type of composite named Fibre Metal Laminates (FML) for making aircraft panels [1]. A GLARE is a GLAss-REinforced composite in the type of FML which was mainly used in Airbus A380 super jumbo in 2001 [22].

Generally, defects are produced during bonding composite of layers with aluminum sheets, handling. Disbonds (air gap) and foreign particles inclusions (intrusion), fibre misalignment, fibre failure, thickness variations, delaminations (DEs) etc. [4] are common failures in FML structures. Delamination (DE) is a mode of defect in FML which exists within the laminate as a cohesive bond. DE is the most common defect in FML which may progress and end-up with fibre-failure. Therefore, DE needs to be properly investigated to aviod further damages in FML structure and safe operation of aircrafts. Usually, this anomality could be identified and characterized by various non-destructive testing and evaluation (NDTE) techniques. Infrared thermography (IRT) is one of NDTE techniques which exercises the abnormal heat distribution over the surface of the specimen to be investigated [16].

Infrared thermography (IRT) is a type of non-destructive technique that exploits the plot of surface temperatures distribution curves to analyse

the subsurface description [21]. IRT is used over many decades to evaluate defects in terms detection, classification and characterisation, such as DEs in layered structures, hidden corrosion in metallic components, cracks in ceramics and metals, voids, impact damage and inclusions in composite materials [13], [18], [7] and [12]. The main objective of this study is to apply the concept of step pulsed active thermography (SPAT) to analyse DE identification sequence in FML used in aircraft panels.

2. Literature Review and Novelty of Investigation

[20] investigated the impact performance of carbon reinforced aluminum laminates (CARAL) by experiments and numerical simulations in which numerical images and results were presented. The active thermography approaches, such as pulsed thermography and vibro-thermography were employed in order to detect simulated DE (inserts), as well as impact damage on GLARE composite panels [8]. Numerical modeling for thermographic inspection of FMLs by both flash pulsed and lock-in thermography [12] was conducted to investigate the detection capabilities. [22] estimated the required heat flux (q) by both analytical and numerical approaches to identify disbonds in FMLs layers under SPAT in thermal reflection (TR) mode. [21] investigated the thermal response of defects such as delaminations and disbonds under through-transmission mode of SPAT and developed empirical formula to obtain the optimum heat requirement and time to identify defects in GLARE type of Fibre metal laminates (FML).

DE parameter effects were analysed using FEM approach in a composite flat plate setup in which DEs were produced using Teflon and other artificial inserts [10] in which the author applied both pulsed and lock-in thermography for the detection of DEs in FML made by E-glass fibre and Aluminium metal laminates using combined experimental and FEM approach [12]. The researcher conducted experiments on GRP pipes for analysing delaminations using step pulsed active thermography [25].

Many investigations were carried to analyse DE behaviour by applying mechanical loading, such as impact load [20], variable amplitude loading [30] and compressive load [23], [17]. Some Few investigations, such as [15], [25], [22] and [21] were investigated composite materials of FML and GRP pipes under SPAT method. The above-mentioned literature [25] analysed DEs in GRP pipes under reflection mode of SPAT. [22] discussed mainly disbonds in FML both analytically and numerically by TR mode of SPAT. [21] investigated that the thermal response of both DEs and disbonds under through-transmission mode of SPAT in IRT. These investigations reported the effectiveness SPAT of IRT to analyse DEs for estimating the required q to its identification based on one mode of observation in a single stack (SS) FML (Al/0^o/90^o/0^o/Al) structures. Based on fore-mentioned literatures, it was found that no specific was carried out at present to analyse DE identification sequence even for SS FML. Therefore, the present investigation was focused to apply both TR and TTT modes of SPAT to investigate DE identification sequence for single stack (SS), double stack (DS) and triple stack (TS) FML numerically through commercially package called ANSYS.

3. IRT Inspection

Basically, the surface temperature of specimen of be investigated is measured in two modes, such as thermal reflection (TR) and thermal through-transmission (TTT). In former mode, the heat source and IR camera are positioned at the same side of specimen and the heat intensity of reflected thermal wave on the surface temperature is continuously monitored. In contrast, TTT mode provides the surface temperature of the specimen by only moving IR camera to the rear surface of FML structure [11] and [21].

The surface temperatures of delaminated and non-delaminated regions were measured by applying continuous heat pulse over the surface of the specimen for a few seconds [13] and [21] in both modes. The identification criteria of 0.1^oC as the desirable temperature difference called thermal contrast (ΔT) to analyse DEs in all stacks of FML due to the maximum resolvable temperature difference (MRTD) for the most of the available thermal imager (IR camera) as 0.1^oC [3].

4. Numerical Modelling

FEM is mostly used to: (i) simulate the behaviour of structures and (ii) conduct a series of parametric analyses in materials containing defects. FEM is more suitable to obtain the solution of complex nonlinear, non-symmetrical mathematical problems governed by partial differential equations, such as one of heat transfer by conduction, convection and radiation with temperature dependent thermal properties of material involved [14].

4.1 Model of FML structure and material properties

(i) SS FML structure:

SS FML is formed by arranging both Al and GRE laminates in the sequence of **Al/90^o/0^o/90^o/Al** shown in Figure 1.

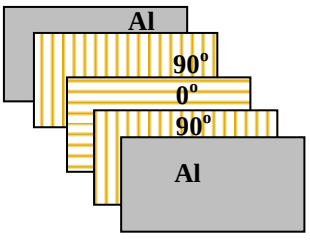

Figure 1 Stacking sequence of SS FML

FML structure of SS is modelled first by modelling three glass-fibre reinforced epoxy (GRE) laminates of 120×70×0.15mm. Second, two aluminium laminates of 120×70×0.3mm were modelled in such a way to cover both top and bottom of GRE laminates, as shown in Figure 2. Third, DE size (S_{DE}) of 10×10mm at 0.45mm and 0.6mm depth with the assumption of artificially induced Teflon film DE of 0.045 mm thick named as DE 1 and DE 2 respectively.

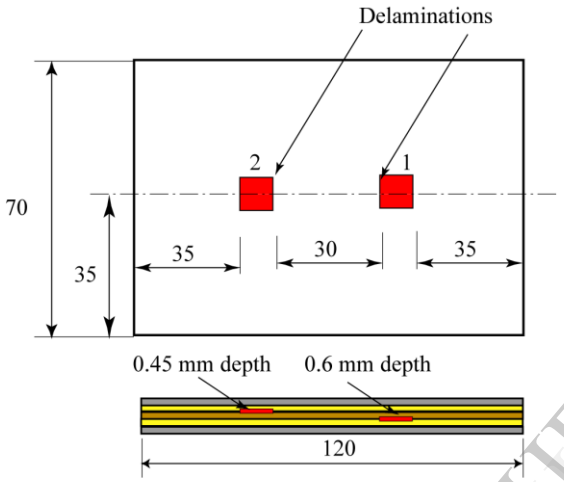

Figure 2 A model of SS FML structure with DEs

The modelled DEs were subtracted using Boolean operations. The same size of DEs was again modelled in such a way to assign Teflon material properties to DEs for the simulation. DE 1 was considered as a near-surface DE and DE 2 was considered as a deeper DE in TR mode but DE 2 and DE 1 were near-surface DE and deeper DE in TTT mode.

(ii) Double stack (DS) FML structure:

Al and GRE laminates are arranged in the order of **Al/90°/0°/90°/Al/90°/0°/90°/Al** to form DS FML shown in Figure 3.

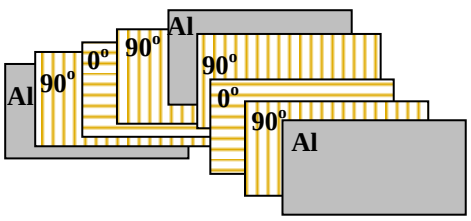

Figure 3 Stacking sequence of DS FML

DS FML structure was modelled by the following steps: (i) modelling SS FML by following the procedure but Al and glass-fibre reinforced epoxy (GRE) laminates are with 200×70×0.15mm, (ii) modelling DE size (S_{DE}) of 10×10mm at 0.45mm and 0.6mm depth named as DE 3 and DE 4 respectively, (iii) modelling the second set of three glass-fibre reinforced epoxy (GRE) laminates of 200×70×0.15mm at the bottom Al laminate, (iv) modelling one Al laminate of 200×70×0.3mm at the bottom of the second set of GRE laminates, and (v) lastly, modelling the second set of S_{DE} of 10×10mm at 1.2mm and 1.35mm depth, shown in Table 2, namely, DE 5 and DE 6.

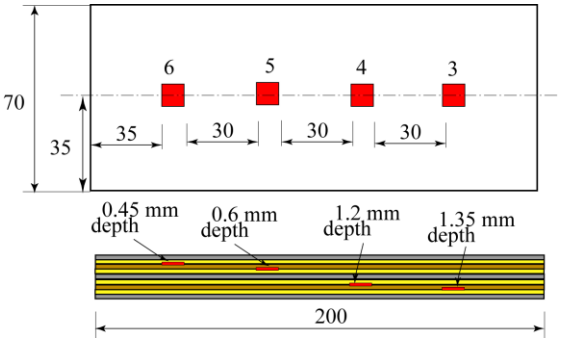

Figure 4 A model of DS FML structure

DE 3 was considered as a near-surface DE and DE 6 was considered as a deeper DE in TR mode but they were opposite in TTT mode.

Table 1 Locations of DE in DS FML Structure

DE No.	Depth, mm	DE No.	Depth, mm
DE 3	0.45	DE 5	1.2
DE 4	0.6	DE 6	1.35

(iii) Triple stack (TS) FML structure:

TS FML is made by stacking both Al and GRE laminates in the sequence of **Al/90°/0°/90°/Al/90°/0°/90°/Al/90°/0°/90°/Al** shown in Figure 5.

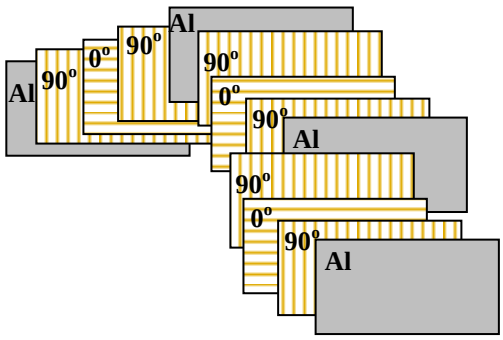

Figure 5 Stacking sequence of TS FML

TS in FML structure was modelled with the size mentioned for GRE and Al laminates in Figure 3 in the same way of DS in FML structure by adding

three more GRE laminates and one Al laminate at the bottom of DS in FML. SDE of 10×10mm were modelled at all possible depths, as mentioned in Table 3.3 which are named from DE7 to DE 12.

Table 2 Locations of DE in TS FML Structure

DE No.	Depth, mm	DE No.	Depth, mm
DE 7	0.45	DE 8	0.6
DE 9	1.2	DE 10	1.35
DE 11	1.95	DE 12	2.1

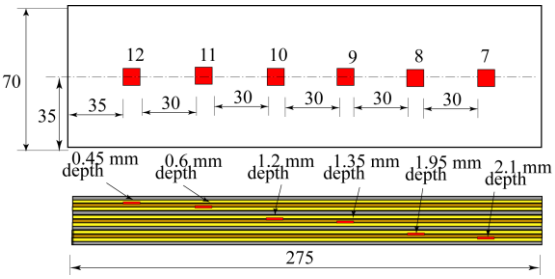

Figure 6 A model of TS FML structure

DE 7 was considered as a near-surface DE and DE 12 was considered as a deeper DE in TR mode they were opposite in TTT mode.

4.2 Thermal Properties of FML Structure and DE

Anisotropic material property conditions were assumed for GRE laminates but Al laminates and DEs (Teflon) were assumed as isotropic materials. The thermal properties of Teflon, Al 2024-T3, and GRE were taken from various literatures [12], [6], [25] and [21]. The properties of GRE at 60% fibre volume fraction which is most commonly used for GRE composite materials were used.

Table 3 Thermal properties of AL 2024-T3, GRE and Teflon

Properties	**Al 2024-T3**	**Glass-fibre epoxy (0^o)**	**Glass-fibre epoxy (90^o)**	**Teflon**
K (W/m^oC)	122.5	1.4	0.8	0.25
C J/kg^oC)	875	840	840	1043
ρ (kg/m^3)	2780	1960	1960	2150

4.3 Element description

All models were meshed using 3D thermal surface elements. SURFACE152 was selected from ANSYS library. The reason of selecting SURFACE152 is that it will be more suitable for any thermal analysis in 3-D. Various loads and surface effects may exist simultaneously. [2].

4.4 Thermal Loading and Boundary Conditions

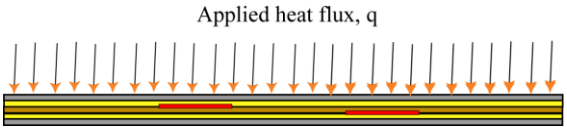

Figure 7 Thermal loading of SS FML with DEs in TR mode

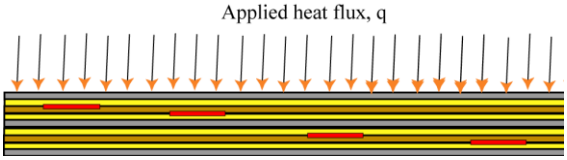

Figure 8 Thermal loading of DS FML with DEs in TR mode

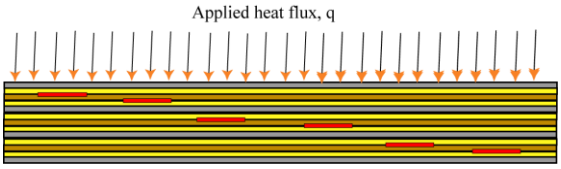

Figure 9 Thermal loading of TS FML with DEs in TR mode

The uniform heat flux (q) 12500 W/m^2 is applied at the top of FML in both modes. The side surfaces and rear surface of the models were considered to be adiabatic [3] and [24] in TR mode, as shown in Figure 7, Figure 8 and Figure 9.

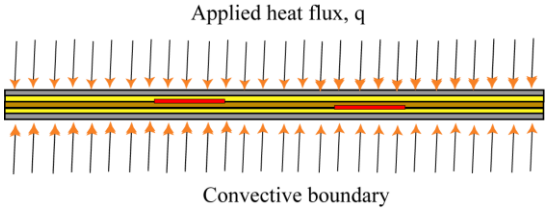

Figure 10 Thermal loading of SS FML with DEs in TTT mode

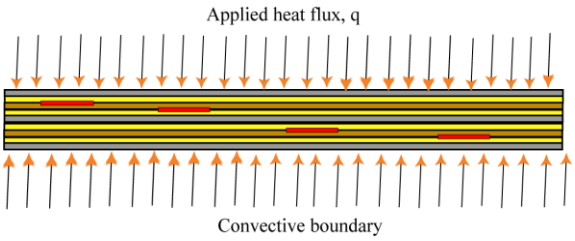

Figure 11 Thermal loading of DS FML with DEs in TTT mode

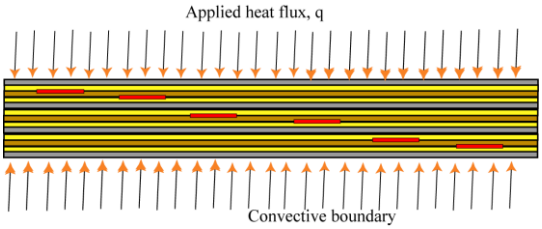

Figure 12 Thermal loading of TS FML with DEs in TTT mode

In TTT mode shown in Figure 10, Figure 11 and Figure 12, the rear surface of the model was subjected to convection boundary with a convection heat transfer coefficient of h = 10W/m^{2}K [21]. Only, the side surfaces of the model were exposed to be adiabatic [10]. The initial temperature of the model was considered same as the atmospheric temperature which is 28^{o}C in both modes.

5. Results and Discussions of DEs

5.1 Analysis of DEs in SS FML structure

The images of SS FML with DEs were obtained from ANSYS simulation shown in Figure 13 and Figure 14 in which the delaminated regions are indicated with different temperatures over non-delaminated region for DE 1 and DE 2 with the applied q of 12500W/m^2 at 1.5 s in both modes. In TR mode, the surface temperature of delaminated region was more than non-delaminated region but it was less than non-delaminated region in TTT mode. As reported in many literatures, ΔT is the temperature difference between delaminated and non-delaminated regions. In the present study, the magnitude of temperature difference was taken as ΔT.

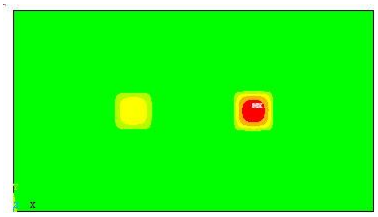

Figure 13 Simulated image of DE 1 and DE 2 in TR mode

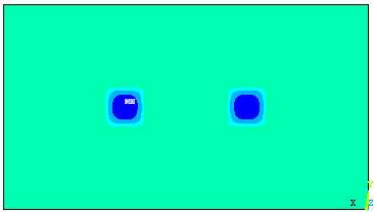

Figure 14 Simulated image of DE 1 and DE 2 in TTT mode

5.1.1 Effect of DE depth on ΔT. Figure 15 shows the variation of DE 1 and DE 2 with τ in TR mode. The results show that the deeper DE 2 produces less ΔT than the near-surface DE 1. For example, DE 2 produces ΔT_{max} of 0.3016^{o}C at τ_{max} of 1.1 sec but 0.1097^{o}C at 1.825 s is produced by DE 2 with the same q. From fore-mentioned results, it is concluded that DE 1 could be identified more quickly with increased ΔT than deeper DE 2. In addition, it is inferred that q required to identify DEs located near the surface is less to reach threshold ΔT of 0.1^{o}C for its effective identification than deeper DEs.

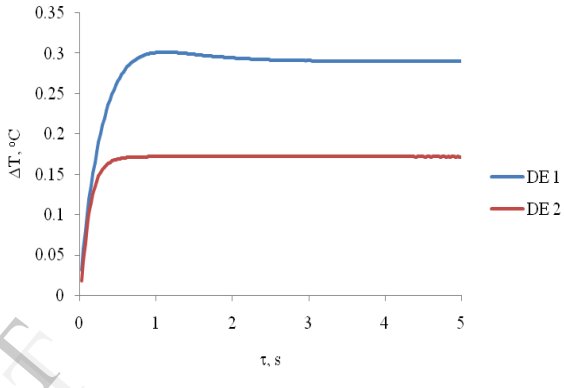

Figure 15 ΔT curves of DE 4 and DE 10 with τ in TR mode

The similar analysis produces the result of deeper DE 1 reporting with increased ΔT in TTT mode. In this case, it is observed that the deeper DE 4 produces more ΔT than near-surface DEs. For example, the deeper DE 1 reaches ΔT_{max} of 0.2961^{o}C at 4.425 s and DE 2 produces ΔT_{max} of 0.1692^{o}C at 3.5 s. Therefore, the results conclude that the near-surface DE 2 could be identified more quickly with reduced ΔT than deeper DE 1 which slightly differs in TR mode. Hence, DE 1 stands first in DE identification sequence followed by DE 2 in TR mode but DE 2 stands first in TTT mode.

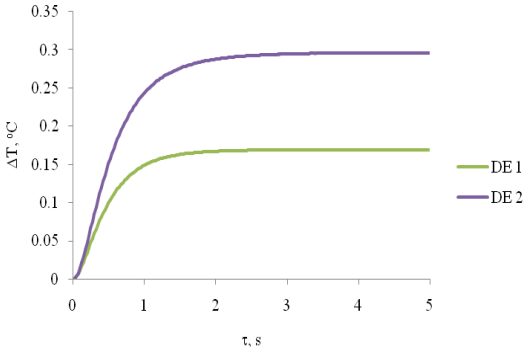

Figure 16 ΔT curves of DE 4 and DE 10 with τ in TTT mode

5.2 Analysis of DEs in a double stack (DS) FML structure

The images of heat distribution of DEs in DS FML for the applied q of 12500W/m^2 at 1.5 s are shown in Figure 17 and Figure 18 for both modes.

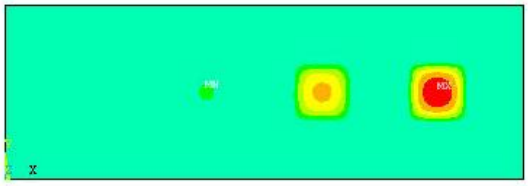

Figure 17 Simulated image of DEs in DS FML in TR mode

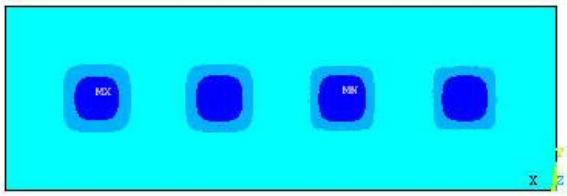

Figure 18 Simulated image of DEs in DS FML in TTT mode

5.2.1 Effect of DE depth on ΔT. The results shown in Figure 19 demonstrate that ΔT of DEs varies with τ at various depths in DS FML under TR mode. ΔT curves of all DEs are almost similar but arranged one over the above based on depth of DEs. As discussed earlier in SS FML structure for near-surface and deeper DEs, the results of DS FML structure report that the deeper DE 6 responds with low ΔT than the near-surface DE 3.

For example, DE 3 produces 0.8343^{o}C at 0.5 sec but 0.6129^{o}C is produced by DE 4 located at 1.35 mm depth. From further reviews on ΔT_{max} to identify DEs in DS FML structure, only, DE 16 reports with insufficient ΔT_{max} (0.0878^{o}C at 4.725 s) for its identification by a thermal imager. Therefore, DE 6 could not be identified with 12500W/m^2 applied in this analysis or it might be identified by applying more heat flux. The order of ΔT_{max} is DE 3, DE, DE 5 and DE6. Further observation on τ_{max}, DE 3, DE 4, DE 5 and DE 6 produce ΔT_{max} at 2.525 s, 2.95 s and 3.4s respectively. Finally, the results conclude that DE 3 is identified first with highest ΔT in its identification sequence followed by DE 4, and DE 5. As per τ_{max} of DE 6, it could be identified at 4.725 s when the sufficient q is applied to reach MRTD. Hence, the study reveals that DE 6 could be identified in DS FML even q applied is more.

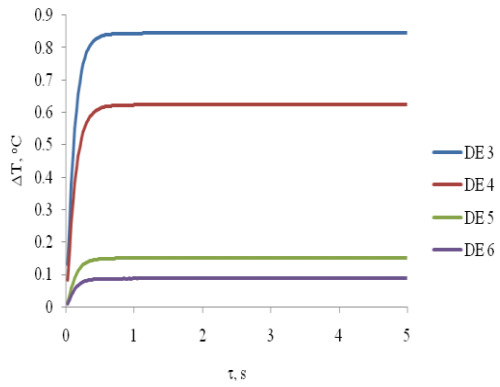

Figure 19 ΔT curves of DS FML structure with τ in TR mode

In TTT mode shown in Figure 20, it is observed that both deeper DE 3 and near-surface DE 6 produce less ΔT than middle DE 4 and DE 5. The results obtained from investigation illustrate that all DEs in TTT mode could be identified with sufficient ΔT. From further investigation on τ_{max}, the study provides that the values of τ_{max} are 5 s, 4.975 s, 4.95 s and 4.95 s for DE 6, DE 5, DE 4 and DE 3 respectively. Therefore, the study concludes that the near-surface DE 6 could be identified later than deeper DE 4 which is in contrast to SS FML. Hence, DE identification sequence is DE 3, DE 4, DE 5 and DE 6.

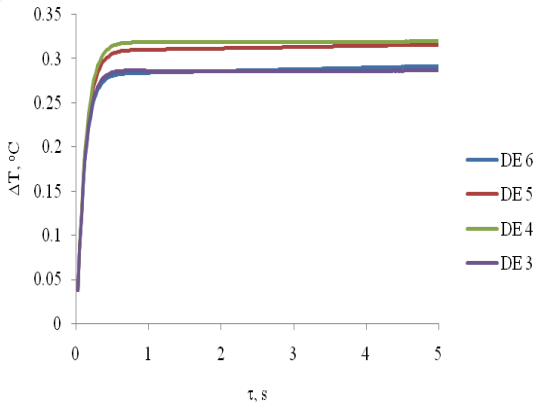

Figure 20 ΔT curves of DS FML structure with τ in TTT mode

5.2.2 Comparison of DEs in SS and DS FML structure. Figure 21 shows the comparison of near-surface and deeper DEs considered in both SS and DS FML under TR mode. ΔT of near-surface DE 3 in DS responds with increased ΔT than the near-surface DE 1 in SS FML. At the same time, ΔT is initially more for DE 6 up to 0.75 s than DE 2 but it is almost closer thereafter. Hence, the results conclude that near-surface DEs of DE 1 and DE 3 make significant changes on ΔT than deeper DE 2 and DE 6. From further analysis, DEs present in SS FML structure whether it may be a near-surface or deeper DE could be identified more

quickly than DEs in DS FML. For example, τ_{max} values of DE 1, DE 3, DE 2, and DE 6 are 1.1 s, 2.525 s, 1.825 s, and 4.725 s respectively. Therefore, DE 1 reports first in DE identification sequence, DE 2 represents the second place, DE 3 stands in the third place followed by DE 6.

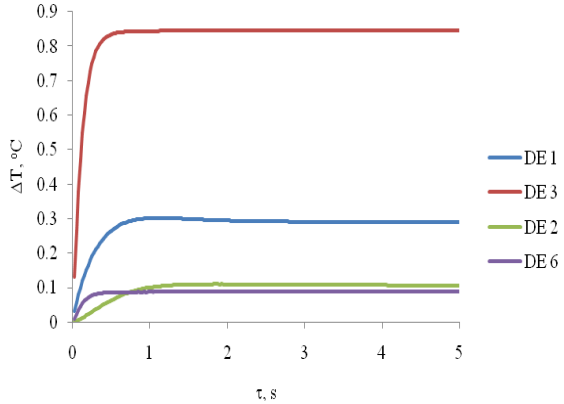

Figure 21 Comparison of near-surface and deeper DEs in both SS and DS FML in TR mode

The comparative results of near-surface and deeper DEs obtained from TTT mode are shown in Figure 22. In TTT mode, it is inferred that the near-surface DE 3 in DS produces more ΔT than other DEs in SS and DEs in DS FML but ΔT produced by DE 2 and DE 3 is almost the same. In this case, ΔT curves of DE 2 and DE 3 do not make much difference. τ_{max} values of DE 1, DE 3, DE 2, and DE 6 are 3.5 s, 4.95 s, 5 s, and 5 s respectively. Therefore, the results arouse the similar conclusion of DEs in DS FML in TR mode by concluding DE 1 standing in the first place in DE identification sequence followed by DE 3, DE 2 and DE 6. By comparison of TR and TTT modes, it is inferred that DE 2 could be identified before DE 3 in TR mode but DE 3 is before DE 2 in TTT mode.

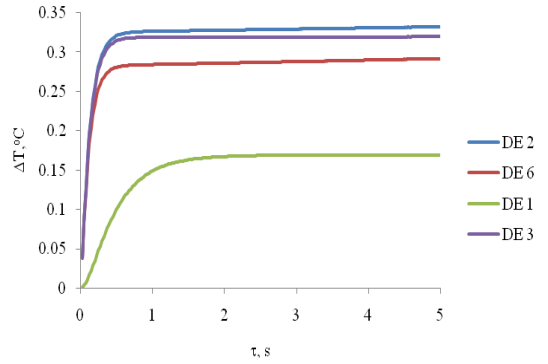

Figure 22 Comparison of near-surface and deeper DEs in both SS and DS FML in TTT mode

5.3 Analysis of DEs in a triple stack (TS) FML structure

ANSYS images of DEs in TS FML for the applied q of 12500W/m^2 at 1.5 s are shown in Figure 23 and Figure 24 in both modes.

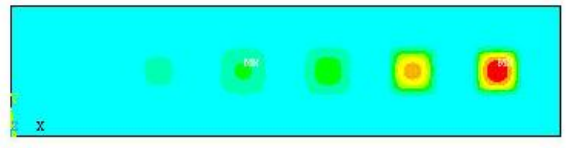

Figure 23 Simulated image of DEs in TS FML for 12000W/m^2 in TR mode

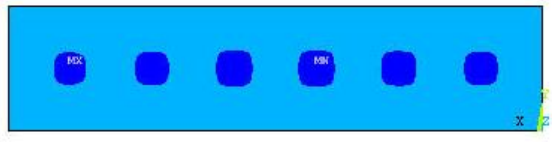

Figure 24 Simulated image of DEs in TS FML for 12500W/m^2 in TTT mode

5.3.1 Effect of DE depth on ΔT. Similar to DS FML, a triple stack (TS) FML was also analysed in the same manner to predict DEs identification sequence at all depths in TR mode. In this case, ΔT curves of all DEs are almost similar and arranged with random spacing. ΔT curve of near-surface DE 7 is placed at the top and arranged in the order of DE 8, DE 9, DE 10, DE 11 and DE 12. The results of TS FML structure reveal that the near-surface DE 7 produces more ΔT than deeper DE 12.

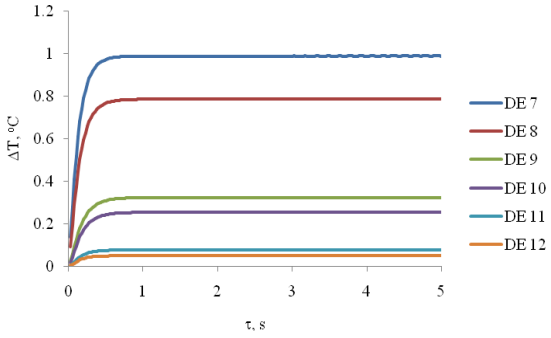

Figure 24 ΔT curves of DEs in TS FML structure with τ in TR mode

For example, DE 7 produces 0.9889^{o}C at 1 sec with applied q of 12500 W/m^2 but 0.7861^{o}C is produced by DE 8 located at 0.6 mm depth for the same q applied. From further investigation on ΔT_{max} to identify DEs in TS FML structure, only, DE 11 and DE 12 are reported with ΔT_{max} of 0.0762^{o}C and 0.0488^{o}C respectively. Therefore, both DE 11 and DE 12 could not be identified or they might be identified by applying more q of 12500W/m^2. In addition, further analysis on τ_{max} from DE 7 to DE 12 presents its values is 2 s, 3.025 s, 4.175 s and 4.275 s respectively. Therefore, DE 7 is identified first, DE 8, DE 9 and

DE 10. Similar to DEs in DS FML, in this case also, DE 11 and DE 12 might be identified by applying more q but they could be identified at almost 5 s.

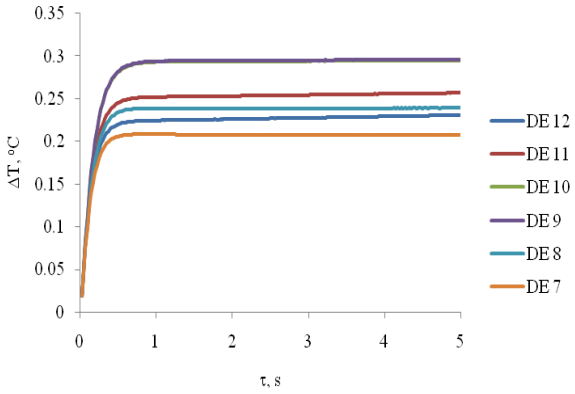

Figure 25 ΔT curves of DEs in TS FML structure with τ in TTT mode

From Figure 25, it is observed that the near-surface DE 12 and DE 11 produce more ΔT than middle and deeper DEs. The results obtained from investigation conclude that all DEs in TS FML structure under TTT mode could be identified with sufficient ΔT. For example, τ_{max} values of DE 12 to DE 7 are 5 s, 5 s, 5 s, 4.925 s, 4.125 s and 0.775 s respectively. From above results, the study confirms that DE 7 could be identified more quickly than DE 8, DE 9, DE10, DE 11 and DE 12 listed in the descending order of DE identification sequence.

5.3.2 Effect of DE depth on ΔT in stacks of FML. The comparison of near-surface and deeper DEs in all stacks of FML structure is shown in Figure 26. The near-surface DE 7 in TS produces the highest ΔT and the near-surface DE 3 in DS reports with the second highest ΔT and so on. The deeper DEs of DE 2, DE 6 and DE 12 do not respond in the similar manner of near-surface DEs. The variation in ΔT is not quiet more to discuss about them individually. Similar to DS FML, the discussion of individual deeper DE could be ignored. From further analysis, DEs present in SS FML structure of a near-surface DE 1 could be identified more quickly than all other DEs in both DS and TS FML. For example, τ_{max} values of DE 1, DE 3, DE 7, DE 2, DE 6 and DE 12 are 1.1 s, 2.525 s, 3.025 s, 1.825 s, 4.725 s, and 1.175 s respectively. Hence, the study concludes that DE 1 stands in the first place to report its presence and other DEs are report one after the other in the sequence of DE 12, DE 2, DE 3, DE 7 and DE 12 respectively.

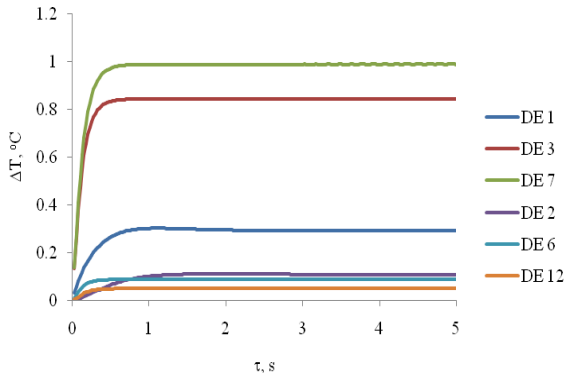

Figure 26 Comparison of near-surface and deeper DEs in all stacks of FML in TR mode

The comparative results of near-surface and deeper DEs obtained from TTT mode are plotted in Figure 26. In TTT mode, it is seen that both deeper and near-surface DEs in DS FML, and near-surface DE 1 produce much more difference on ΔT than TS FML and DE 2 but the variation of DEs located in DS FML does not produce significant values. Therefore, the individual discussion on both near-surface and deeper DEs in DS FML could be ignored. For example, τ_{max} values of DE 1, DE 3, DE 2, DE 6, DE 7 and DE 12 are 3.5 s, 4.95 s, 5 s, 5 s, 4.95 s and 4.975 s respectively. Therefore, the results provoke the similar conclusion of DEs in TS FML in TR mode by confirming DE 1 standing in the first place in DE identification sequence and the rests follow the order of DE 3, DE 7, DE12, DE 2 and DE 6 .

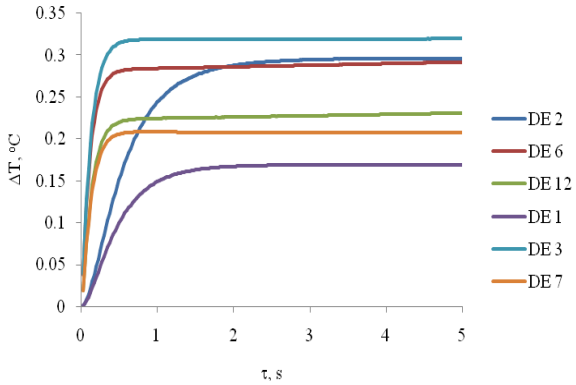

Figure 27 Comparison of near-surface and deeper DEs in all stacks of FML in TTT mode

6. Conclusions

In the present investigation, the sequence of delamination identification was analysed in all SS, DS and TS FML structures. The results conclude that SPAT in TR mode is more suitable for identifying near-surface DEs and TTT mode is more suitable for identifying deeper DEs. DEs located in SS in both modes could be identified

easily. The analyses of DS and TS FML structures were carried out to analyse DEs located at various depths. The results reveal that the surface temperature DEs increases when number of stacks of FML is increased.

The numerical results of DEs in both DS and TS FML structures conclude that DE 16, DE 21 and DE 22 in TR mode could not be identified in this investigation but they DEs could be easily identified with sufficient MRTD in TTT mode.

It concludes the near-surface DE 1 located in SS FML could be identified first with reduced ΔT than both DS and TS FML structures in modes. Thus, the results conclude that SPAT of IRT could effectively be applied to investigate the DEs identification sequence.

7. Nomenclature

ρ	Density, kg/m^3
τ	Pulse duration, s
τ_{max}	Time to maximum ΔT, s
ΔT	Thermal contrast, ^oC
ΔT_{max}	Thermal contrast, ^oC
C	Specific heat, J/kgK
h	Convective heat transfer coefficient, W/m^{2}K
K	Thermal conductivity, W/mK
q	Heat flux, W/m^2
q_{opt}	Optimum heat flux, W/m^2
s_{DE}	Size of delamination, mm or m
T_{DE}	Time to identify delaminations, s

8. References

[1] Ad Vlot and Jan Willem Gunnink, "*Fibre Metal Laminates": An Introduction.* Kluwer Academic Publishers. Springer Netherlands, 2001.

[2] ANSYS, *ANSYS Heat Transfer Manual* for Release 10, 2005.

[3] Avdelidis N. P and Almond D.P, "Transient thermography as a through skin imaging technique for aircraft assembly Modelling and experimental results", *Journal of Infrared Phys. Technol*., Vol. 45. No. 2, pp. 103-114, 2004.

[4] Avdelidis N.P, Almond D.P, Dobbinson A, Hawtin B.C, Ibarra-Castanedo C and Maldague X, "Aircraft composites assessment by means of transient thermal NDT", *Progress in Aerospace Sciences*, Vol. 40, pp 143–162, 2004.

[5] Edson C, Rogério A, Luiz C, and Mirabel C, "A Review on the Development and Properties of Continuous Fiber/epoxy/aluminum Hybrid Compositesfor Aircraft Structures", *Journal of Material Research*, Vol. 9. No. 3, pp. 247-256, 2006.

[6] Hagenbeek M, "Characterisation of Fibre Metal Laminates under Thermo- mechanical Loadings". PhD thesis. Faculty of Aerospace Engineering, 2005, *Delft University of Technology*, pp 224.

[7] Ibarra-Castanedo C, Grinzato E, Marinetti S, Bison P, Genest M, Grenier M, Jean-Marc Piau, Bendada A and Maldague X, "Recent progresses in the inspection of aerospace components by infrared thermography" *17th World Conference on Nondestructive Testing*, 2008, *Shanghai, China*, pp.25-28.

[8] Ibarra-Castanedo1 P, Avdelidis N.P, Grinzato G, Paolo G, Sergio M, Claudiu P, Abdelhakim B and Maldague X, "Delamination detection and impact damage assessment of GLARE by active thermography", *International Journal of materials and Product Technology*, 2011, Vol. 41, pp. 5-16.

[9] Khan S.U., Alderliesten R.C., and Benedictus, R. "Delamination in Fiber Metal Laminates (GLARE) during fatigue crack growth under variable amplitude loading", J. of Fatigue, Vol. 33. No.9, pp 1292–1303, 2011.

[10] Krishnapillai M, Jones R, Marshall I.H, Bannister M, and Rajic N, "NDTE using pulse thermography: Numerical modeling of composite subsurface defects", *J. Composite Structures*, Vol. 75, pp. 241-249, 2006.

[11] Lugin S and Netzelmann U, "A defect shape reconstruction algorithm for pulsed thermography", *NDT&E International*, Vol. 40, pp. 220–228, 2007.

[12] Mabrouki F, Genest M, Shi G and Fahr A, "Numerical modeling for thermographic inspection of fibre metal laminates", *J. NDT and E International*, Vol. 42, pp. 581-588, 2009.

[13] Maldague X, "*Theory and practice of infrared technology for nondestructive testing*"Wiley-Interscience, *New York*. 453 – 525, 2001.

[14] Mirela S, Ibrarra-Castanedo, Maldague X, Bendada A, Svaic S and Boras I, "Pulse thermography applied on a complex structure sample: comparison and analysis of numerical and experimental results", *IV conferencia Panamericana de END, Buenos Aires*, 2007.

[15] Muralidhar C and Arya N.K, "Evaluation of defects in axisymmetric composite structures by thermography", *NDT&E International*, Vol. 26. No. 4, pp. 198-193, 1993.

[16] Muzia G, Rdzawski Z.M, Rojek M, Stabik J and Wróbel G, "Thermographic diagnosis of fatigue degradation of epoxy-glass composites", *Journal of Achievements in Materials and Manufacturing Engineering*, Vol. 24. No. 2, pp. 123-126, 2007.

[17] Naganarayana B. P. and Atluri S. N. "composite plates under strength reduction and delamination growth in thin and thick composite plates under compressive loading" J. of Computational mechanics, Vol. 6, pp 170-189, 1995.

[18] Omar M, Haassan M, Donohue K, Saito K and Alloo R, "Infrared thermography for inspecting the adhesion integrity of plastic welded joints", *NDT and E International*, Vol. 39, pp. 1-7, 2006.

[19] Rene Alderliesten, "On the Development of Hybrid Material Concepts for Aircraft Structures", *Journal of Recent Patents on Engineering*, Vol. 3. No. 3, pp 25-38, 2009.

[20] Song S.H,. Byun Y.S, Ku T.W, Song W.J, Kim J and Kang B.S "Experimental and Numerical Investigation on Impact Performance of Carbon Reinforced Aluminum Laminates" J. Mater. Sci. Technol., Vol. 26. No.4, pp 327-332, 2010.

[21] Sundaravalli S, Majumder M and Vijayaraghavan G.K "Numerical Analysis of Defects in FML using Through-Transmission Mode of Active Thermography", *Journal of Engineering Trends and Technology*, Vol. 3. No. 3, pp 437-447, 2012.

[22] Sundaravalli S, Vijayaraghavan G.K. and Majumder M.C. "Estimation of required heat input

for the evaluation of Disbonds in FMLs Using Thermography", *International Conference on Modeling, Optimization and Computing* (ICMOC 2010), National Institute of Technology, Durgapur, India, October 28 - 30, 2010, American Institute of Physics (AIP) Conference Proceedings, Vol. 1298, pp 129-134. ISBN: 978-0-7354-0854-8

[23] V´ıt Obdr˘z´alek, Jan Vrbka, "On buckling of a plate with multiple delaminations", J. engineering mechanics, Vol. 174. No. 1, pp. 37–47, 2010.

[24] Vijayaraghavan G.K. and Sundaravalli S "Evaluation of Pits in GRP Composite Pipes by Thermal NDT Technique". *Journal of Reinforced Plastics and Composites*, 30 (19), pp 1599–1604, 2011.

[25] Vijayaraghavan G.K. Majumder M.C. and Ramachandran K.P. 2010. Quantitative Analysis of Delaminations in GRP Pipes Using Thermal NDTE Technique. *Journal of Advanced Research in Mechanical Engineering*, Vol. 1. No. 1, pp.60-68.

ACKNOWLEDGMENT

The authors would like to acknowledge Dr. Benny Jospeh, Principal, Vimal Jothi Engineering College, Kerla India, for his kind cooperation & support to provide for the valuable guidelines extended to collect literatures about FML.

BIOGRAPHICAL NOTES

S.Sundaravalli is currently working as a Faculty in the Department of Mechanical engineering, M.A.M College of Engineering, Trichy, India. An M. Tech in Energy Technology from the Pondicherry engineering College, Pondicherry, she has around fourteen years of teaching experience and currently pursuing Ph D in the National Institute of Technology, Durgapur, India. She has authored 8 text books, such as Engineering Thermodynamics, Design jigs, fixtures and press tools, Manufacturing technology II, Automobile engineering, Renewable sources of energy etc.,

Dr. M C Majumder is a Professor in the Department of Mechanical Engineering and Member Secretary of the Senate, National Institute of Technology, Durgapur, India. He has a PhD from the Indian Institute of Technology, Kharagpur, India. He has guided many Ph D scholars. His prime area of research is Tribology.

Dr. G.Manikandan is currently working as a Professor in the Department of Mechanical engineering, Velammal College of Engineering and technology, Madurai, India. He has a PhD from Anna University, Chennai, India. He has guided many Ph D scholars. He has authored 1 text book, such as Rejuvenating Acceptance Sampling Plan ISBN 978-3-8443-8230-3. His prime area of research is quality engineering and management.

Dr. G.K.Vijayaraghavan is currently working as a Principal with Mechanical engineering, Cauvery College of Engineering and Technology, Trichy, India. An M. Tech in Machine Design from the Indian Institute of Technology, Madras, he has around Fifteen years of teaching experience and pursed Ph D in the National Institute of Technology, Durgapur, India. He has authored 14 text books including Design of machine elements, Design jigs, fixtures and press tools, Manufacturing technology, Thermal engineering and Mechatronics.